ISSN 1392 - 1207. MECHANIKA. 2010. Nr.4(84)

The model of bent threaded connection in three segments

A. Krenevičius*, Ž. Juchnevičius, M. K. Leonavičius*****
**Vilnius Gediminas Technical University, Saulėtekio al. 11, 10223 Vilnius, Lithuania, E-mail: kron@fm.vgtu.lt*
***Vilnius Gediminas Technical University, Saulėtekio al. 11, 10223 Vilnius, Lithuania, E-mail: ma@fm.vgtu.lt*
****Vilnius Gediminas Technical University, Saulėtekio 11, 10223 Vilnius, Lithuania,*
E-mail: mindaugas.leonavicius@vgtu.lt

1. Introduction

The analysis of load distribution in the threads is a prerequisite for determining stress concentration and fatigue durability of the threaded connection which can be subjected not only to axial force but also simultaneously to bending moment. In engineering practice, the loading is usually asymmetric or eccentric and this causes bending moments to be applied to structures or to it's elements such as rods and the threaded joints also [1-6].

The experimental study of the effect of bending directly on the distribution of stresses along the helix of the thread root by using photoelastic models is presented in [6]. However in analytical detailed calculations of the stud fatigue strength the turn loads and the loads in cross-sections of stud/bolt core are determining primarily and then the stresses in turn roots [7]. Previous analytical analysis of the load distribution in threads due to multiple loading which includes bending moments and also axial and tangential forces is presented in [8]. However here this is performed without estimation of turn deflections influence on bolt core and nut wall displacements. In the article [9] the equation for the compatibility of bent threaded connection elements' displacement and analytical solution of this equation are obtained from the fundamental theory of elasticity. Here, the threaded connection presents one segment model of full profile turns which disregards runouts in the nut.

For more accurate analysis of load distribution along the thread due to bending of the threaded connection it is useful to estimate the influence of runouts also. The most interest occurs in the case of coarse-pitch thread. Then the both runouts are located in a great part of the nut. That is close to the third part in the standard nut length.

This paper describes a modification to the theory given in [9] and models the threaded connection by three longitudinal segments. The first and third segments here represent runouts where turns have partial engagment (Fig. 1).

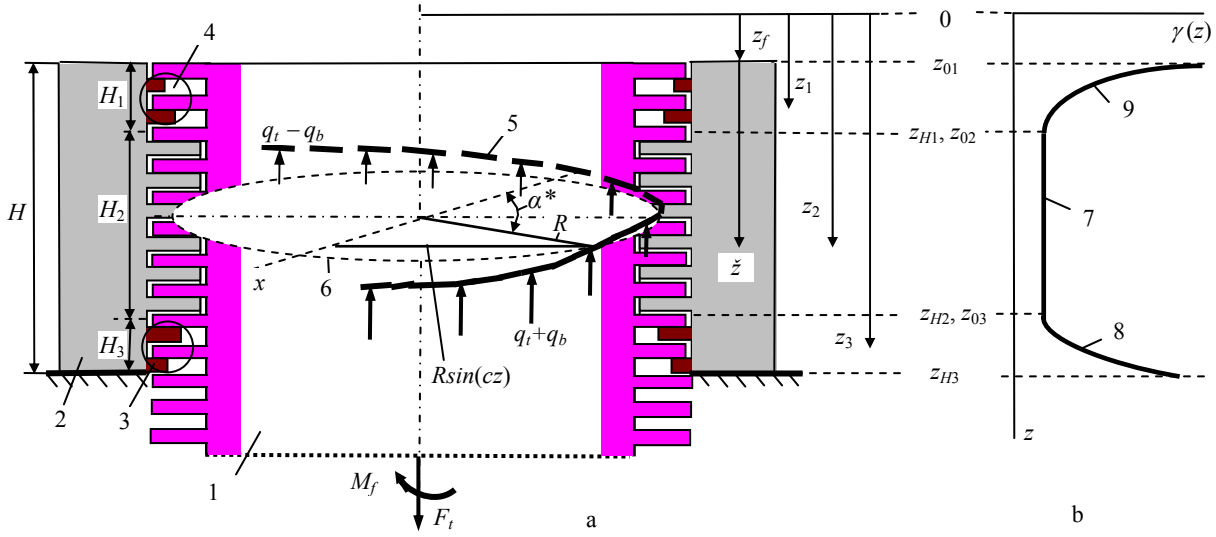

Fig. 1 Scheme of threaded connection: a – loading of threaded connection: *1* - stud, *2* - nut, *3* and *4* - runouts, *5* - helix of the stud thread pitch diameter, *6* - cross-section of the stud; b – turn pairs pliability graph: *7* - pliability of the fully engaged turns, *8* and *9* - turn pair pliabilities in runouts

2. Positions of threaded connection elements

In the present model a threaded connection is divided into three segments i ($i = 1; 2; 3$) which pliabilities of turn pairs are described by separate functions (Fig. 1). Pliability of the turns in the middle segment H_2 is constant ($\gamma(z_2) = \gamma = \text{const}$). Contact depth of the stud and nut turns within the segments H_1 and H_3 (in runouts) varies (Fig. 1, b). Therefore the pliability of the turn pair here varies also ($\gamma(z_1) \neq \text{const}$, $\gamma(z_3) \neq \text{const}$). The length of these segments is equal to the thread pitch: $H_1 = P$ and $H_3 = P$.

In the model the origin of any cross-section location coordinate $z = z_i$ ($i = 1; 2; 3$) is receded from the free end of the nut on a phase length z_f, which is designed to set a position of the threaded connection with respect to longitudinal axis thus with respect to bending plane also. So the coordinate z of any cross-section always is linked with its distance $\check{z}$ from the free end of the nut by equality $z = z_f + \check{z}$. Position for any thread helix point now can be expressed by turning angle α (which is equal to α^* shown in Fig. 1)

in the following way

$$\alpha = \frac{2\pi}{P} z = cz \tag{1}$$

Chanching of the phase length value z_f gives a possibility to set position of the bottom runout origin with respect to bending plane by the value of z_{03}. This is necessary because turn pairs near the bearing surface of the nut are mostly loaded in the area around z_{03} and can be in various positions. The four specific positions (positions *I*, *II*, *III*, *IV* where $sin(cz_{03}) = 1, 0, 0, -1$) of the threaded connection in respect to bending plane are shown in Fig. 2.

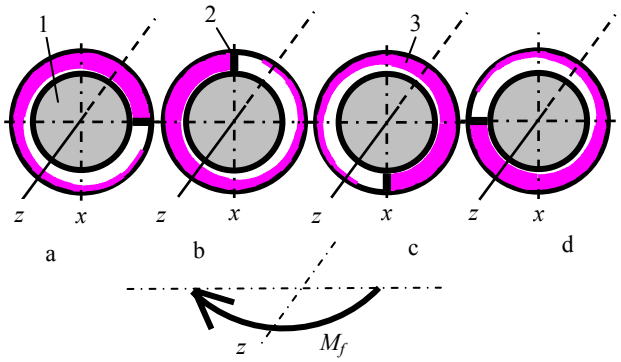

Fig. 2 Specific positions of runout at the bearing surface of nut: a, b, c, d – *I*, *II*, *III*, *IV* runout positions: *1* - stud core, *2* - runout origin, *3* - turns contact area in runout

3. Differential equation for turn deflections

External load of the threaded joint can be schematized by two main components. It is axial load of tightening F_t and external bending moment M_f (Fig. 1, a). Therefore on turns of the stud and nut in opposite directions arise equal distributed longitudal load intensities $q_t(z)$ and $q_b(z)$ caused by tightening and bending respectively (Fig. 1). Due to the action of these loads the proportional turn pair deflections $\delta_t(z)$ and $\delta_b(z)$ occur (Fig. 3)

$$\delta_t(z) = \gamma(z) q_t(z), \qquad \delta_b(z) = \gamma(z) q_b(z) \tag{2}$$

The relations of these turn pair deflections to the stud and the nut cross-sections displacements are shown in Fig. 3.

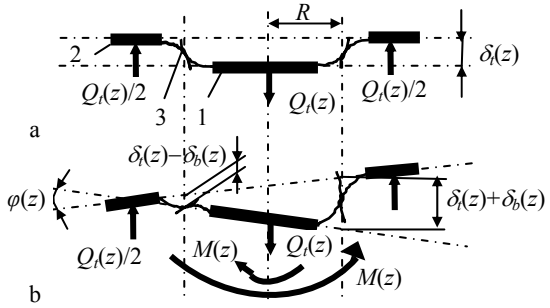

Fig. 3 Displacements of the threaded connection elements: a – due to tightening; b – due to tightening and bending; *1*, *2* - cross-sections of the stud and the nut, *3* - turn pair

Last-mentioned displacements are caused by internal axial force $Q(z)$ and internal moment $M(z)$ which even act to the stud core and to the nut wall but in opposite direction. The load intensity $q_t(z)$ and turn pair deflection $\delta_t(z)$ caused by tightening can be calculated by the method given in [10]. Further there are analysed regularities of the load intensity $q_b(z)$ and the turn pair deflection $\delta_b(z)$ due to bending only as was desined to present in this paper.

It is seen in Fig. 3 that turn pair deflection has relation with inter-deviation of the stud and nut cross-sections. The compatibility of displacements of these elements in any segment *i* of threaded connection can be expressed by the following equation

$$\varphi_s(z) + \varphi_n(z) \approx \frac{\delta_b(z)}{R\,sin(cz)} - \frac{\delta_b(z_0)}{R\,sin(cz_0)} \tag{3}$$

where $\varphi_s(z) \approx tan\varphi_s(z)$ and $\varphi_n(z) \approx tan\varphi_n(z)$ are deviations of the stud and nut cross-sections, $z = z_i$, $z_0 = z_{0i}$ is coordinate of the segment *i* origin.

According to the theory of elasticity the deviations of the stud and nut cross-sections are

$$\varphi_s(z) = \int_{z_0}^{z} \frac{M(z)}{E_s I_s} dz \tag{4}$$

$$\varphi_n(z) = \int_{z_0}^{z} \frac{M(z)}{E_n I_n} dz \tag{5}$$

where E_s and E_n, I_s and I_n are modulus of elasticity and moments of inertia of the cross-sectional area for the stud core and the nut wall respectively.

Bending moment in cross-section of any segment by using Eq. (2) and certain designation could be expressed in the following forms

$$M(z) = M(z_0) + \int_{z_0}^{z} m(z)dz = M(z_0) + \int_{z_0}^{z} q_b(z) R\,sin(cz)dz \tag{6}$$

$$M(z) = M(z_0) + R\int_{z_0}^{z} \frac{y(z)}{\gamma(z)} sin^2(cz)dz \tag{7}$$

$$y(z) = \frac{q_b(z)}{\gamma(z)\,sin(cz)} = \frac{\delta_b(z)}{sin(cz)} \tag{8}$$

where $m(z)$ is local moment due to $q_b(z)$ [8] and $y(z)$ is the function which expresses variation of turn pair deflection amplitude.

Now by using Eqs. (4), (5), (7), (8) the Eq. (3) was rewrited in the other form and differentiated two times. Hereby were found

$$R\lambda M(z_0) + R^2\lambda \int_{z_0}^{z} \frac{y(z)}{\gamma(z)} sin^2(cz)dz = y'(z) \tag{9}$$

$$\gamma(z) y''(z) - R^2 \lambda y(z)\,sin(z) = 0 \tag{10}$$

where $\lambda = 1/(E_s I_s) + 1/(E_n I_n)$.

The next equation which can be used to express the boundary conditions for any segment *i* at $z = z_{0i}$ and $z = z_{Hi}$ is obtained from Eqs. (7), (9)

$$M(z) = \frac{1}{R\lambda} y'(z) \tag{11}$$

Because the turns pliability in the middle segment H_2 is constant and in runouts (in segments H_1 and H_3) it is variable the differential Eq. (10) must be solved separate.

4. Analytical solution for middle segment H_2

In segment H_2 of the threaded connection $\gamma(z_2) = \gamma = \text{const}$. Therefore the differential Eq. (10) can be rewrited

$$y''(z) - by(z)\sin(z) = 0 \tag{12}$$

where $b = R^2\lambda/\gamma$ is constant factor.

The approximate analytical solution of Eq. (12) was postulated in the next form

$$y(z_2) = A_2 \sinh(nz_2) + B_2 \cosh(nz_2) \tag{13}$$

Further factor n of Eq. 13 must be find. At first after substitution of $y'(z_2)$ in Eq. (11) the next expression for certain mean bending moment was got

$$M_m(z_2) = \frac{A_2 n}{R\lambda}\cosh(nz_2) + \frac{B_2 n}{R\lambda}\sinh(nz_2) \tag{14}$$

Another expression for bending moment was got after substituting of Eq. (13) into Eq. (7) and after integrating within it

$$\begin{aligned} M(z_2) = {} & \frac{A_2 R}{\gamma}\frac{1}{n^2+4c^2}\left[n\cdot\cosh(nz_2)\sin^2(cz_2) - \right. \\ & \left. - c\cdot\sinh(nz_2)\sin(2cz_2) + (2c^2/n)\cosh(nz_2)\right] + \\ & + \frac{B_2 R}{\gamma}\frac{1}{n^2+4c^2}\left[n\cdot\sinh(nz_2)\sin^2(cz_2) - \right. \\ & \left. - c\cdot\cosh(nz_2)\sin(2cz_2) + (2c^2/n)\sinh(nz_2)\right] \end{aligned} \tag{15}$$

To determine expression for factor n was used equality of Eqs. (14) and (15), i.e., $M_m(cz^*) = M(cz^*)$. When $cz^* = k_1(P/4)$, where $k_1 = 0, 1, 3, 5..$, and when $cz^* = k_2(P/2)$, where $k_2 = 0, 1, 2, 3..$, from this equality were obtained two expressions respectively

$$n = \sqrt{0.5\left[-(4c^2 - b) + \sqrt{16c^4 + b^2}\right]} \tag{16}$$

$$n = \sqrt{-2c^2 + c\sqrt{4c^2 + 2b}} \tag{17}$$

Both these expressions give practically the same value of the factor n. For example, in the case of connection M16×2 the values of this factor are $n = 0.15640$ and $n = 0{,}15630$. In the sixth chapter numerically it is shown that the value of n defined by using Eq. (16) is right for all values of z, not only for z^*.

Thus, the analytical solution for segment H_2 express Eq. (13) (to find $\delta_b(z_2)$ and $q_b(z_2)$ from Eq. (8)) and Eq. (15) to find $M(z_2)$.

The factors A_2 and B_2 of Eqs. (13) and (15) can be found by using boundary conditions of all segments together.

5. Analytical solutions for runouts

In the runouts, i.e., in segments H_1 and H_3 of the threaded connection $\gamma(z_i) \neq \text{const}$ ($i = 1$ or 3). The variation of the turn pair pliability in length of any runout was described by the following formula

$$\gamma(z_i) = V_i e^{u_i z_i} \tag{18}$$

where V_i and u_i are constant factor and power exponent which can be defined according to the tensile test results of the turn' pairs, egaged over the incomplete profile [10]. They have been defined by using the known fully engaged turns' pliabilities in one edge of segment H_1 or H_3 where $\gamma(z_{H1}) = \gamma$ and $\gamma(z_{03}) = \gamma$, and also the experimental turns' pliability factors in the middle of these segments. By using data given in [10] the corresponding ratio was determined: $\gamma(z_{H1} - P/2)/\gamma \approx 1.67$ or $\gamma(z_{03} + P/2)/\gamma \approx 1.67$.

The approximate analytical solution of differential Eq. (10) for runouts was postulated in the following form

$$\begin{aligned} y(z_i) &= A_i e^{n_{Ai} z_i}(n_{Ai} z_i + W_{Ai}) + B_i e^{n_{Bi} z_i}(-n_{Bi} z_i + W_{Bi}) = \\ &= A_i f_{Ai}(z_i) + B_i f_{Bi}(z_i) \end{aligned} \tag{19}$$

where n_{Ai}, W_{Ai}, n_{Bi} and W_{Bi} are the factors which need to find, f_{Ai} and f_{Bi} are designations (further indexes $A_i = A$, $B_i = B$ at $i = 1$ and $i = 3$).

At first after substitution of $y'(z)$ in Eq. (11) the next expression for certain fictional bending moment was obtained

$$\begin{aligned} M^*(z_i) &= A_i \frac{f'_A(z_i)}{R\lambda} + B_i \frac{f'_B(z_i)}{R\lambda} = \\ &= A_i \frac{n_A e^{n_A z_i}(n_A z + W_A + 1)}{R\lambda} + B_i \frac{n_B e^{n_B z_i}(-n_B z + W_B - 1)}{R\lambda} \end{aligned} \tag{20}$$

Another expression for bending moment for runouts was obtained after substituting of Eqs. (18) and (19) into Eq. (7) and after integrating within it

$$\begin{aligned} M(z_i) &= M(z_{0i}) + \int_{z_{0i}}^{z_i} \frac{\left[A_i f_A(z_i) + B_i f_B(z_i)\right]}{V_i e^{u_i z_i}} R\sin^2(cz_i)dz_i = \\ &= A_i F_A(z_i) + B_i F_B(z_i) \end{aligned} \tag{21}$$

where $F_A(z_i)$ and $F_B(z_i)$ are designations which can be expressed in the following common form

$$\begin{aligned} F_\omega(z) = {} & \frac{Re^{tz}}{2V}\left[\pm\frac{n_\omega(tz-1)}{t^2} \mp n_\omega\left(\left(tz - \frac{t^2-4c^2}{p}\right)\frac{\cos(2cz)}{p} - \right.\right. \\ & \left.\left. - \left(\frac{4ct}{p} - 2cz\right)\frac{\sin(2cz)}{p}\right) - \frac{W_\omega}{p}\left(t\cos(2cz) + 2c\sin(2cz)\right) + \right. \\ & \left. + \frac{W_\omega}{t}\right] \end{aligned} \tag{22}$$

where $\omega = A_i$ or $\omega = B_i$, $t = t_\omega = n_\omega - u_i$, $V = V_i$, $p = p_\omega = t^2 +$

$+ 4c^2$, $z = z_i$, $i = 1$ or $i = 3$; where are dual signs the upper sign is valid at $\omega = A_i$ and the under sign is valid in the case of $\omega = B_i$.

To determine four unknown factors n_{Ai}, W_{Ai}, n_{Bi} and W_{Bi} was used equality of Eq. (20) to Eq. (21) i.e., $M^*(cz_i^*) = M(cz_i^*)$ at $z_i^* = z_{0i} + P/4$ and $z_i^* = z_{Hi} - P/4$. The factors n_{Ai} and W_{Ai} for any runout can be solved from the equations system

$$\frac{f'_A(z_{0i} + P/4)}{R\lambda} = F_A(z_{0i} + P/4) \qquad (23)$$

$$\frac{f'_A(z_{Hi} - P/4)}{R\lambda} = F_A(z_{Hi} - P/4) \qquad (24)$$

Further in analogous way the factors n_{Bi} and W_{Bi} can be solved from similar equations system also

$$\frac{f'_B(z_{0i} + P/4)}{R\lambda} = F_B(z_{0i} + P/4) \qquad (25)$$

$$\frac{f'_B(z_{Hi} - P/4)}{R\lambda} = F_B(z_{Hi} - P/4) \qquad (26)$$

These two systems authors solved numerically by using the suite of mathematical programs Maple-9. By numerical experiments authors persuaded that it is enough to have coincidence of the functions $M^*(cz_i^*)$ and $M(cz_i^*)$ in two points only and that chosen coordinates z_i^* give the most calculation results accuracy of the load distrbution in runouts.

Thus, the analytical solution for segments H_1 and H_3 (where $i = 1$ or $i = 3$) express Eq. (19) (to find $\delta_b(z_i)$ and $q_b(z_i)$ from Eq. (8)) and Eq. (21) to find $M(z_i)$.

Eventually unknown factors A_i and B_i for all three segments (now $i = 1, 2, 3$) can be found by using the system of equations, which expresses all segment's boundary conditions

$$\delta(z_{0i}) = \delta(z_{H(i-1)}),\ M(z_{0i}) = M(z_{H(i-1)})$$

$$M(z_{01}) = 0,\quad M(z_{H3}) = M_f. \qquad (27)$$

6. Calculation results

The calculation of load distributions along the threads first has been made by using the approximate analytical method given in the chapters 3, 4 and 5. The objects of this calculation were threaded connections M16×2, M16×1.5, M16×1, M52×4 and M110×6 with compressed nut (height of the nut $H = 0.8d$) – made from grade 25X1MΦ steel.

Then the differential Eq. (10) writed for both runouts and differential Eq. (12) for the middle segment of threaded connection were solved separate numerically by Runge–Kutta method. (It was realized by using the suite of mathematical programs Maple-9). For this the same boundary conditions $M(z_{0i})$ of every segment obtained in the analytical solution were used. The calculation results are presented with reference to the real coordinate $\check{z} = z - z_f$ of the cross-section of threaded connection in Figs. 4-7.

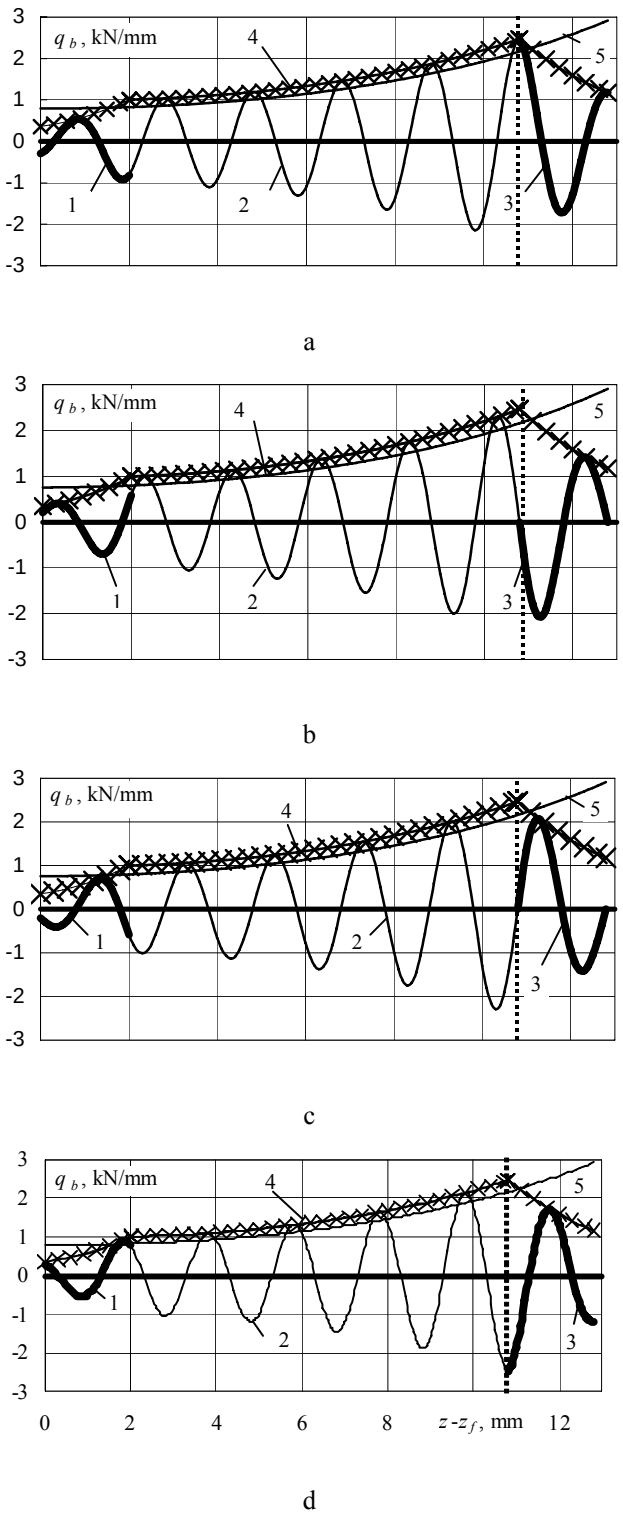

Fig. 4 Loads distribution in bent threaded joint M16×2: a, b, c, d - *I*, *II*, *III*, *IV* bottom runout positions; analytical solutions: *1*, *3* - $q_b(z)$ in runouts, *2* - $q_b(z)$ in middle segment, *4* - $y(z)/\gamma(z)$, *5* - $y(z)/\gamma(z)$ for model without runouts, × - numerical solutions of $y(z)/\gamma(z)$, dashed line – cross-section at z_{03}–z_f

Average indices of mechanical properties of conections grade 25X1MΦ steel: proof strength $R_{p0.02} = 860$ MPa, tensile strength $R_m = 1010$ MPa, percentage area of reduction of tension specimen $Z = 60.2\%$, module of elasticity $E = 210$ GPa.

Pliabilities for one turn pair (made from grade

25X1MΦ steel) for every thread were established experimentally by the technique given in [10]: $\gamma = 3.78\times10^{-3}$; 4.37×10^{-3}; 7.31×10^{-3}; 3.54×10^{-3} and 3.26×10^{-3} mm/(kN/mm) for threads M16×2, M16×1.5, M16×1, M52×4 and M110×6 respectively.

The calculations of turn load amplitude function $y(z)/\gamma(z)$, $q_b(z)$ and $M(z)$ for connections M16, M52 and M110 have been performed at external bending moment M_f applied to the studs which values caused the ratio of nominal maximal normal stresses in the stud with the proof strength to be $\sigma_{b,nom,max}/R_{p0.02} = 0.31$. For threaded connections M16×2 the total turn loads and total local stresses in stud thread have been determined also. In this case the turn loads and local stresses due to tightening have been obtained at $\sigma_{t,nom,max}/R_{p0.02} = 0.6$ from the method presented in [10], which gives the possibility to estimate the influence of runouts.

The calculation results given in Figs. 4-6 show the serviceability of the three segments analytical model to estimate position, pitch and size of threaded connection subjected to bending.

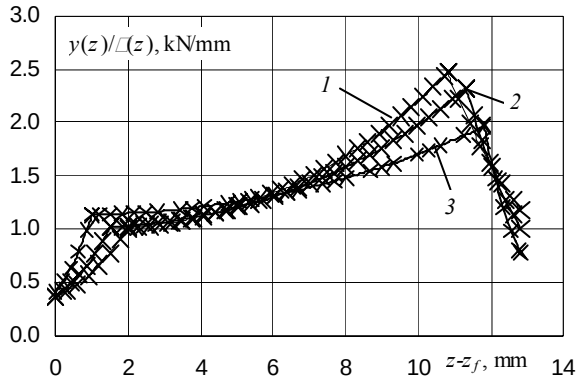

Fig. 5 Turn load due to bending amplitude functions for threaded connections M16 in position *I*: *1* – $P = 2$ mm , *2* – $P = 1.5$ mm, *3* – $P = 1$ mm; lines - analytical solutions, × - numerical solutions of Eqs. (10, 12)

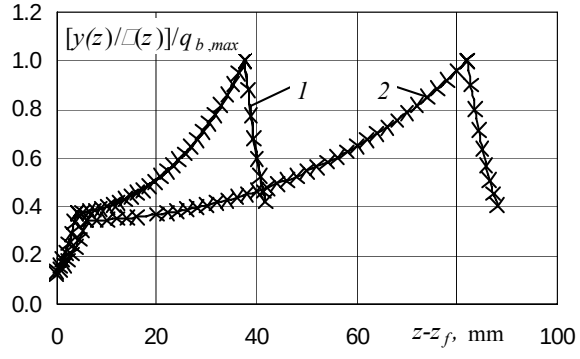

Fig. 6 Relative turn load due to bending amplitude functions: *1* – M52×4 in position *I*, *2* – M110×6 at position I, lines - analytical solutions, × - numerical solutions of Eqs. (10 and 12)

In Fig. 7 the variation of the internal bending moment $M(z)$ in stud M16×2, which has been calculated by using three segments analytical model (Eqs. (15 and 21)) is shown also.

The values of turn load (due to bending) amplitude functions and $M(z)$ obtained by Runge-Kutta method in Figs. 4, 5, 6, 7 are shown by criss-cross. These values differ from corresponding values obtained by analitical method less than by 1%.

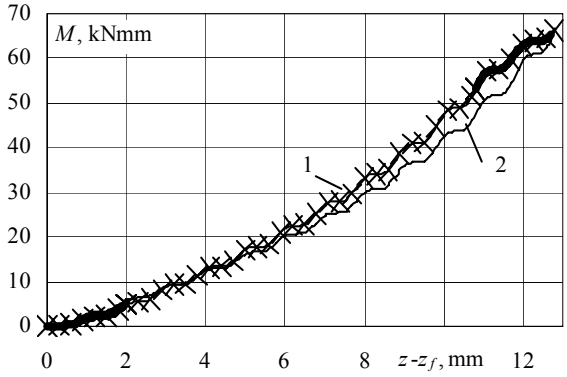

Fig. 7 Bending moment distribution in threaded joint M16×2 in position *I*: *1* – with estimating of runouts, *2* – model without runouts, lines - analytical solutions, × - numerical solutions of Eqs. (10 and 12)

As at the worst the maximal turn load location found after tightening in the stud (aproximately at $z \approx z_{03}$) is in it's bending plane and coincides with the location of the maximum turn load caused by bending. This occurs when the threaded connection is in position *I*. The ditribution of the total turn loads for this connection position is presented in Fig. 8.

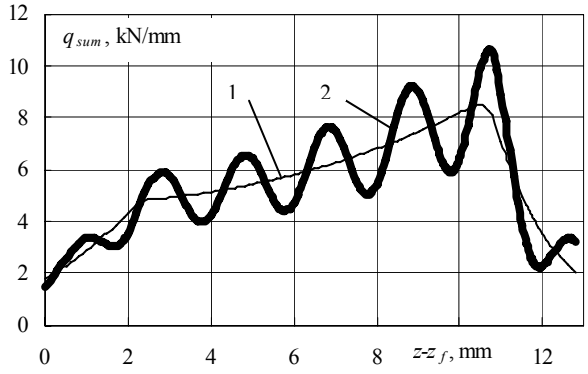

Fig. 8 Load distribution along the thread in connection M16×2 at position *I*: *1* – turn loads $q_t(z)$ due to tightening, *2* – $q_{sum}(z) = q_t(z) + q_b(z)$; $H = 12.8$ mm

In strength calculation norm for nuclear equipments [11] the fatigue durability is estimating according the local conditional elastic stresses σ^*. These stresses for axial loaded stud thread which arise at tightening were calculated by using the following formula [1]

$$\sigma_t^*(z) = \frac{q_t(z)P}{f}K_{m,t} + \frac{Q_t(z)}{A_s}K_{0,t} \qquad (28)$$

here $K_{0,t}$, $K_{m,t}$ are concentration factors of stresses due to the axial force $Q_t(z)$ and the stud turn load $q_t(z)$ respectively; A_s is cross-sectional area of the stud core; f is the turn's contact surface projection into the plane, perpendicular to the stud axis; P is the thread pitch. The values of

elastic stresses concentration factors, defined in work [1] are: $K_{0,t} = 2$ and $K_{m,t} = 1{,}95$, at the turns' root rounding-up radius being $R = 0.144P$.

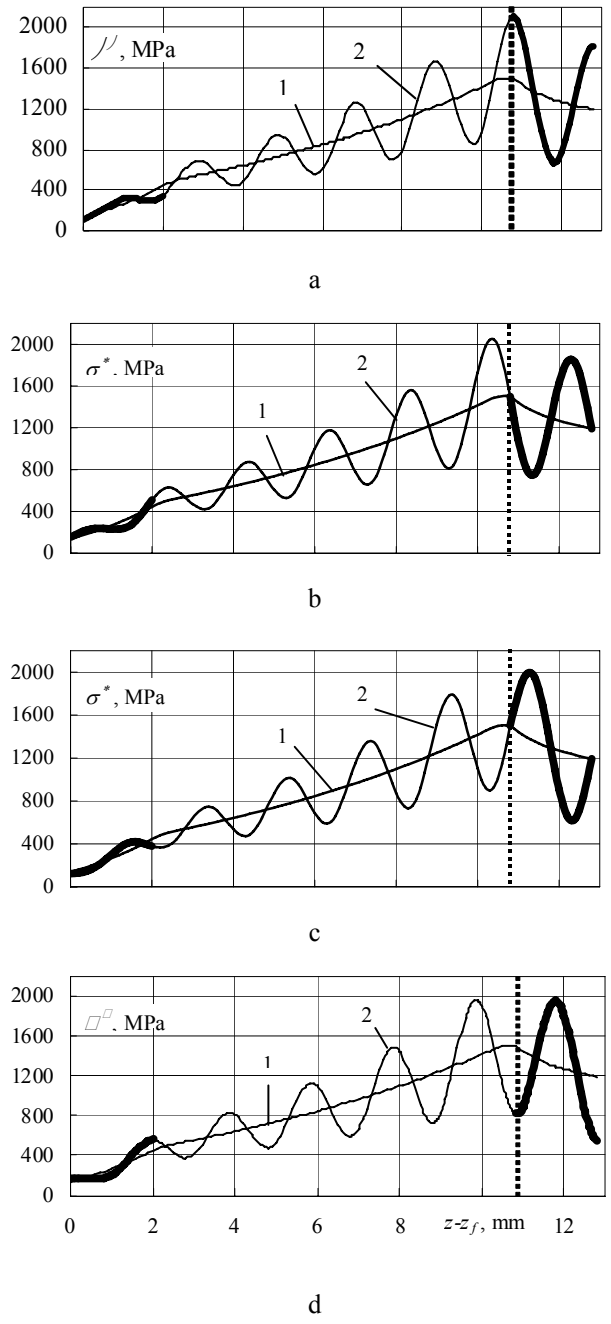

Fig. 9 Distribution of local conditional stresses along the thread in stud M16×2: a, b, c, d – *I*, *II*, *III*, *IV* positions of connection; *1* - $\sigma_t^*(z)$ due to tightening, *2* – total local stresses $\sigma_\Sigma^*(z)$; dashed line – cross-section at z_{03}–z_f; $H = 12.8$ mm

The conditional elastic stresses in stud thread due to bending were calculated on the analogy of Eq. (28)

$$\sigma_b^*(z) = \frac{q_b(z)P}{f} K_{m,b} + \frac{M(z)R\sin(cz)}{I_s} K_{0,b} \qquad (29)$$

here $K_{0,b} \approx k_r K_{0,t}$ and $K_{m,b} \approx K_{m,t}$ are concentration factors of the stresses due to bending moment $M(z)$ and the stud turn load $q_b(z)$ respectively; k_r is factor which estimates difference between the local stresses in the stud at bending and at it's tension; here was assumed $k_r \approx 0.9$ after analysis of concentration factors of the notched rods.

The total local stresses in the thread of the stud are

$$\sigma_\Sigma^*(z) = \sigma_t^*(z) + \sigma_b^*(z) \qquad (30)$$

Distribution of local conditional stresses along the thread in stud M16×2 for connection positions *I*, *II*, *III*, *IV* are shown in Fig. 9. The stress $\sigma_\Sigma^*(z)$ as $q_{sum}(z)$ have maximum at position *I* of connection (aproximately at $z \approx z_{03}$). At the position *IV* it has minimum value, which is by 8% less than that at connection position *I*.

For comparison purpose the local stresses $\sigma_\Sigma^*(z)$ for the stud thread M16×2 have been calculated also by using one segment model where runouts are neglected (Fig. 10).

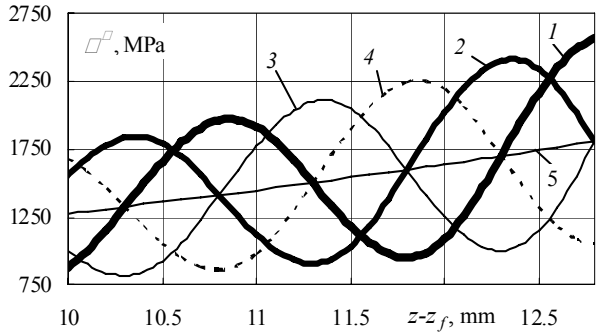

Fig. 10 Distribution of local conditional stresses along the thread in stud M16×2 according to one segment model: 1, 2, 3, 4 – total local stresses $\sigma_\Sigma^*(z)$ at connection positions *I*, *II*, *III*, *IV*, *5* – local stresses $\sigma_t^*(z)$ due to tightening; $H = 12.8$ mm

In this case the stud total local stresses $\sigma_\Sigma^*(z)$ have maximum at the connection being in position *I* but at $z = z_{H3}$ (on curve *1* in Fig. 10). This maximum value is by 21% greater than that in the case of three segments model (on curve *2* in Fig. 9, a). The maximum value of the stud local stresses due to bending $\sigma_b^*(z)$ is by 22% greater in the case of one segment model also (at connection position *I* and at $z = z_{H3}$) than that in the case of three segments model (at connection position *I* and at $z \approx z_{03}$).

7. Conclusions

1. The differential equation for the compatibility between deflections of the partly engaged turn pair and deviations of the stud and nut cross-sections in runouts of the threaded connection subjected to bending is derived. The approximate analytical solution of this equation is proposed also.

2. For the bent threaded connection the designed three segments model gives a possibility to estimate the influence of the runouts and of the connection position

upon the load distribution along the thread. The turn load calculation results for the threaded connections M16, M52 and M110 obtained by using approximate analytical solutions and obtained by using numerical Runge-Kutta method differ very slight – less than 1%.

3. In dangerous cross-sections the maximum and minimum values of the greatest total local stresses in stud threads occur when threaded connection is in the positions *I* and *IV* respectively. These values differ by 8% in the case of threaded connection M16×2 considered by using three segments model.

4. The maximum thread local stresses σ_{Σ}^{*} and σ_{b}^{*} in the stud at its' beeing in the position *I* and determined by using three segments model are noticeably less than these stresses in the case of one segment model. The both differences of the maximum stresses of σ_{Σ}^{*} and of the maximum stresses of σ_{b}^{*} obtained for the threaded connection M16×2 exceed 20%.

References

1. **Machutov, N.A., Stekolnikov, V.V., Frolov, K.V., Prigorovskij, N.I.** Constructions and Methods of Calculation of Water-Water Power Reactors. -Moscow: Nauka, 1987.-232p. (in Russian).
2. **Leonavičius, M., Šukšta, M.** Shakedown of bolts with a one-sided propagating crack. -Journal of Civil Engineering and Management. -Vilnius: Technika, 2002, vol.VIII, Nr.2, p.104-107.
3. **Tumonis, L., Schneider, M., Kačianauskas, R., Kačeniauskas, A.** Comparison of dynamic behavior of EMA-3 railgun under differently induced loadings. -Mechanika. -Kaunas: Technologija, 2009, Nr.4(78), p.31-37.
4. **Atkočiūnas, J., Merkevičiūtė, A., Venskus, A., et al.** Nonlinear programming and optimal shakedown of frames. -Mechanika. -Kaunas: Technologija, 2007, Nr.2(64), p.27-33.
5. **Daunys, M., Bazaras, Z., Timofeev, B.** Low cycle fatigue of materials in nuclear industry. -Mechanika. -Kaunas: Technologija, 2008, Nr.5(73), p.12-17.
6. **Burguete, R., Patterson, E.** The effect of eccentric loading on the stress distribution in thread roots. -Fatigue. Fracture of Engineering Materials. Structures. 1995, vol.18, No. 11, p.1333-1341.
7. **Patterson, E.** A Comparative study of methods for estimating bolt fatigue limits. -Fatigue and Fracture of Engineering Materials and Structures, 1990, v.13, No1, p.59-81.
8. **Yazawa, S., and Hongo, K.** Distribution of load in screw thread of a bolt-nut connection subjected to tangential forces and bending moments. -JSME International Journal, 1988, Series I, vol.31, No.2, p.174-180.
9. **Krenevičius, A., Juchnevičius, Ž.** Load distribution in the threaded joint subjected to bending. -Mechanika. -Kaunas: Technologija, 2009, Nr.4(78), p.12-16.
10. **Selivonec, J., Krenevičius, A.** Distribution of load in the threads. -Mechanika. -Kaunas: Technologija, 2004, Nr.2(46), p.21-26.
11. Norm for Calculation of Nuclear Power Equipments and Pipelines Strength. -Moscow: Energoatomizdat, 1989.-525p. (in Russian).

A. Krenevičius, Ž. Juchnevičius, M. K. Leonavičius

TRIJŲ RUOŽŲ LENKIAMOS SRIEGINĖS JUNGTIES MODELIS

R e z i u m ė

Straipsnyje pateiktas trijų ruožų lenkiamos srieginės jungties modelis apkrovų pasiskirstymui sriegyje apskaičiuoti. Modelis leidžia įvertinti jungties kraštinių vijų, sukibusių ne visu profiliu, ir jungties padėties lenkimo plokštumos atžvilgiu įtaką. Sudarytos lenkiamos srieginės jungties elementų poslinkių suderinamumo lygtys. Nustatyti jų sprendiniai – skaitiniai ir apytiksliai analitiniai.

A. Krenevičius, Ž. Juchnevičius, M. K. Leonavičius

THE MODEL OF THE BENT THREADED CONNECTION IN THREE SEGMENTS

S u m m a r y

For the calculation of load distribution between turns the threaded connection subjected to bending is modeled by three segments. The model gives a possibility to estimate the influence of runouts and of the connection position with respect to bending plane. The equations for the displacements compatibility of threaded joint elements for every segment are constructed. The numerical and approximate analytical solutions for these equations are obtained.

А. Кренявичюс, Ж. Юхнявичюс, М. К. Ляонавичюс

МОДЕЛЬ ИЗГИБАЕМОГО РЕЗЬБОВОГО СОЕДИНЕНИЯ

Р е з ю м е

В статье представлена модель изгибаемого резьбового соединения, которое схематизированного тремя участками. Модель предназначена для расчета распределения нагрузок по виткам соединения и дает возможность учитывать как влияние крайних, выходящих из зацепления витков соединения, так и влияние положения резьбового соединения по отношению к плоскости изгибающего момента. Для каждого участка составлены уравнения совместимости перемещений элементов изгибаемого резьбового соединения. Получены соответствующие дифференциальные уравнения и их решения – численные и приближенные аналитические.

Received March 27, 2010
Accepted July 2, 2010